

# Clinical EEG and Neuroscience

<http://eeg.sagepub.com/>

---

## Neurofeedback Training Induces Changes in White and Gray Matter

J. Ghaziri, A. Tucholka, V. Larue, M. Blanchette-Sylvestre, G. Reyburn, G. Gilbert, J. Lévesque and M. Beauregard

*Clin EEG Neurosci* published online 26 March 2013

DOI: 10.1177/1550059413476031

The online version of this article can be found at:

<http://eeg.sagepub.com/content/early/2013/03/19/1550059413476031>

---

Published by:



<http://www.sagepublications.com>

On behalf of:



EEG and Clinical Neuroscience Society

**Additional services and information for *Clinical EEG and Neuroscience* can be found at:**

**Email Alerts:** <http://eeg.sagepub.com/cgi/alerts>

**Subscriptions:** <http://eeg.sagepub.com/subscriptions>

**Reprints:** <http://www.sagepub.com/journalsReprints.nav>

**Permissions:** <http://www.sagepub.com/journalsPermissions.nav>

>> [OnlineFirst Version of Record](#) - Mar 26, 2013

[What is This?](#)

# Neurofeedback Training Induces Changes in White and Gray Matter

Clinical EEG and Neuroscience  
00(0) 1-8  
© EEG and Clinical Neuroscience  
Society (ECNS) 2013  
Reprints and permission:  
sagepub.com/journalsPermissions.nav  
DOI: 10.1177/1550059413476031  
eeg.sagepub.com



J. Ghaziri<sup>1</sup>, A. Tucholka<sup>2</sup>, V. Larue<sup>1</sup>, M. Blanchette-Sylvestre<sup>1</sup>,  
G. Reyburn<sup>1</sup>, G. Gilbert<sup>2</sup>, J. Lévesque<sup>1</sup>, and M. Beauregard<sup>1,2,3</sup>

## Abstract

The main objective of this structural magnetic resonance imaging (MRI) study was to investigate, using diffusion tensor imaging, whether a neurofeedback training (NFT) protocol designed to improve sustained attention might induce structural changes in white matter (WM) pathways, purportedly implicated in this cognitive ability. Another goal was to examine whether gray matter (GM) volume (GMV) might be altered following NFT in frontal and parietal cortical areas connected by these WM fiber pathways. Healthy university students were randomly assigned to an experimental group (EXP), a sham group, or a control group. Participants in the EXP group were trained to enhance the amplitude of their  $\beta 1$  waves at F4 and P4. Measures of attentional performance and MRI data were acquired one week before (Time 1) and one week after (Time 2) NFT. Higher scores on visual and auditory sustained attention were noted in the EXP group at Time 2 (relative to Time 1). As for structural MRI data, increased fractional anisotropy was measured in WM pathways implicated in sustained attention, and GMV increases were detected in cerebral structures involved in this type of attention. After 50 years of research in the field of neurofeedback, our study constitutes the first empirical demonstration that NFT can lead to microstructural changes in white and gray matter.

## Keywords

neurofeedback, structural magnetic resonance imaging, white matter, gray matter, sustained attention

Received September 24, 2012; revised 17 December 2012; accepted January 4, 2013.

## Introduction

Neurofeedback is an operant conditioning procedure in which individuals learn to recondition their brain activity. There is mounting evidence that EEG-based NFT can improve attentional performance in individuals with attention deficit hyperactivity disorder (ADHD).<sup>1,2</sup> With respect to this issue, we have previously demonstrated, in children with ADHD, that increasing  $\beta 1$  frequency band (through NFT) can enhance the activity in brain regions involved in various attentional processes.<sup>3,4</sup>

To date, a few EEG investigations have shown that  $\beta$  activity is associated with sustained attention.<sup>5,6</sup> This construct refers to the top-down cognitive ability to maintain attention to a specific stimulus or location over prolonged periods of time.<sup>7</sup> Clinical studies indicate that damage to frontal and parietal areas, primarily but not exclusively in the right hemisphere, leads to sustained attention impairment.<sup>8</sup>

Findings from the recent diffusion tensor imaging (DTI) studies suggest that cognitive training can induce measurable changes in white matter architecture. For instance, Takeuchi and colleagues<sup>9</sup> have shown in young, healthy individuals that working memory training can increase fractional anisotropy (FA)—which is thought to reflect microstructural properties of WM such as myelination, axon caliber, and fiber density<sup>10</sup>—in WM

areas adjacent to brain regions critically involved in this form of memory. In addition, Lee et al.<sup>11</sup> have found that long-term trained Baduk players, relative to inexperienced controls, exhibit increased FA values in brain areas implicated in cognitive functions required to play this Korean game.

Along the same lines, there is also evidence that cognitive training can lead to structural GM changes. In regard to this question, Ceccarelli et al.<sup>12</sup> scanned 32 students at baseline, and after 2 weeks using MRI. The students were divided into 2 groups, 13 defined as “students in cognitive training” (ie, they underwent a 2-week learning period) and 19 “students not in

<sup>1</sup>Centre de Recherche en Neuropsychologie et Cognition (CERNEC), Département de Psychologie, Université de Montréal, Montreal, Canada

<sup>2</sup>Centre de recherche du Centre hospitalier de l'Université de Montréal (CRCHUM) and MR Clinical Science, Philips Healthcare, Cleveland, OH, USA

<sup>3</sup>Département de Radiologie, Université de Montréal, Montreal, Canada

## Corresponding Author:

Mario Beauregard, Département de Psychologie, Mind/Brain Research Lab (MBRL), Centre de Recherche en Neuropsychologie et Cognition (CERNEC), Université de Montréal, C.P. 6128, succursale Centre-Ville, Montréal, Québec, Canada H3C 3J7.

Email: mario.beauregard@umontreal.ca

cognitive training” (ie, they were not involved in any learning activity). The GM changes were measured using tensor-based morphometry. At follow-up, the students in cognitive training compared to students not in cognitive training, had a significant GMV increase in cortical regions involved in cognition. This finding indicates that cognitive learning produces short-term structural changes in brain’s GM.

In view of the results of the neuroimaging studies conducted by Ceccarelli et al.<sup>12</sup>, Lee et al.<sup>11</sup> and Takeuchi et al.<sup>9</sup>, we decided to perform an exploratory MRI study to investigate whether a NFT protocol designed—in principle—to improve sustained attention might induce structural changes in WM pathways, purportedly implicated in this cognitive ability. The FA values of these pathways were assessed using DTI. A secondary objective of this study was to examine whether GMV might be altered following NFT in frontal and parietal cortical areas connected by these WM fiber pathways. Voxel-based morphometry (VBM) was used to address this issue.

## Materials and Methods

### Participants

Thirty students from University of Montreal (mean age: 22.2; standard deviation [SD]: 2.4; range: 18-30), with no history of neurological or psychiatric disorders, were recruited. Participants were randomly assigned to an experimental group ([EXP], NFT;  $n = 12$ , 9 females; mean age: 22.4; SD: 1.6), a sham group ([SHAM],  $n = 12$ , 9 females; mean age: 22.0; SD: 3.1), or a control group ([CON]; to control for the passage of time;  $n = 6$ , 3 females; mean age: 20.7; SD: 1.0).

### The NFT Protocol

Participants in the EXP group were trained to enhance the amplitude of their  $\beta_1$  activity (15-18 Hz) in the right hemisphere. A double channel montage was used with a total of 5 electrodes, 1 on each ear lobe, the ground electrode on the tragus, and the 2 main electrodes at F4 and P4. According to the 3-dimensional (3D) probabilistic anatomical craniocerebral correlation via the international 10/20 System, F4 corresponds to the right middle and superior frontal gyri, while P4 corresponds to the right superior parietal lobule (SPL).<sup>13</sup> The relevant frequencies were extracted from EEG recordings and fed back, using an audiovisual online feedback loop in the form of a video game. A sampling rate of 128 Hz with 2-second epochs was utilized. The NFT was conducted over a period of 13.5 weeks (40 sessions, 3 training sessions per week). Each session was subdivided in 10 tryouts of 3 minutes (first 20 first sessions) and 6 tryouts of 5 minutes (last 20 sessions). Each session lasted for 30 minutes. The NFT was provided using the Procomp 2 and Biograph software (version 5.1.2, Thought Technology Ltd, Montreal, Canada).

Before starting the sessions, the impedance of the electrodes was checked and had to be below 5 k $\Omega$ . Sessions started with a 1-minute recording at rest that was used as a comparison measure and as an objective to beat during the tryouts. This

procedure was also used to determine the training threshold. On the computer screen, 2 columns were displayed, representing the EEG activity of the electrodes at F4 and P4, respectively. Participants could choose a song and an animated image from a list, which were later used as feedback information. On the left side of the screen, F4 feedback was shown, and when the activity was above the threshold, the column turned green and the animation was played; when the activity was under the threshold, the column turned red and the animation was stopped. The P4 feedback was provided on the right side of the screen. When the activity was above the threshold, the column turned green and the song was played; when the activity was under the threshold, the column turned red and the song stopped playing. Participants had to find their own mental strategies to self-regulate their EEG activity. During each session, technicians motivated participants and gave them tips regarding their progression after each tryout. Depending on the participants’ results, the animation could be changed and the threshold could be increased to keep the NFT demanding.

The sham NFT was also conducted over a period of 13.5 weeks (40 sessions, 3 training sessions per week). Participants in the SHAM group were trained following the exact same protocol as the NFT group, except that they received the feedback of registered sessions from members of the EXP group (each member of the SHAM group was randomly paired to a member of the EXP group). Technicians also motivated the participants in both the EXP and the SHAM groups. Participants in both the EXP and the SHAM groups were asked not to consume coffee, tea, or energy drinks at least 3 hours before NFT. Participants in the CON group did not receive any intervention.

### The MRI Data Acquisition

We acquired the data on a 3-T Achieva scanner (Philips, the Netherlands). The diffusion-weighted images were acquired with a single-shot spin-echo echo-planar pulse sequence (TR = 7.96 milliseconds; TE = 77 milliseconds; flip angle = 90°; slices = 68; field of view = 230 mm; matrix = 128  $\times$  126; voxel resolution = 1.8 mm  $\times$  1.8 mm  $\times$  1.8 mm; readout bandwidth = 19.6 Hz/pixels; echo-planar imaging direction bandwidth = 1572.5 Hz; 8-channel head coil; SENSE acceleration factor = 2). One pure T2-weighted image ( $b = 0$  second/mm<sup>2</sup>) and 60 images with non-collinear diffusion gradients ( $b = 1500$  second/mm<sup>2</sup>) were obtained. In addition, T1-weighted images were acquired using 3D T1 gradient echo (scan time = 8.11 minutes; TR = 8.1 milliseconds; TE = 3.8 milliseconds; flip angle = 8°; slices = 176; voxel size = 1 mm  $\times$  1 mm  $\times$  1 mm). The MRI data were obtained at Time 1 (ie, 1 week before the beginning of NFT or sham treatment) and Time 2 (ie, 1 week after the end of NFT or sham treatment).

### White Matter/Diffusion Data

Data were preprocessed, using the Diffusion Toolbox (FDT, v.2.0) from the FSL package (version 4.1, www.fmrib.ox.ac.uk/fsl). Diffusion data were corrected for eddy-current

distortions and head motion using affine registration to the nondiffusion-weighted volume ( $b = 0$ ). Brain extraction tool (BET)<sup>14</sup> was used to remove nonbrain tissue (ie, skull and scalp<sup>15</sup>) from the nondiffusion-weighted volume and to create a brain mask. The FA map was obtained by fitting a tensor model to the corrected diffusion data at each voxel.

Voxel-wise analysis of multiparticipant diffusion data was performed using Tract-Based Spatial Statistics.<sup>16</sup> First, nonlinear registration was applied on all FA images to a  $1 \times 1 \times 1$  mm standard space. The target image was automatically chosen from the most representative participant in the study. It was then affined-aligned into the Montreal Neurological Institute (MNI)152 standard space. Next, every image was transformed by combining the nonlinear transform to the target FA image with the affine transform from that target to MNI152 space. Mean FA was thresholded to  $>0.2$  to remove non-WM tissues. The resulting image was then skeletonized to represent the most common WM pathways. The skeletonization procedure aimed at improving the interindividual WM registration. Then the FA map of each participant was projected on the mean-FA skeleton, resulting in a 4-dimensional skeletonized FA image. Next, for each group, the data acquired at Time 1 and Time 2 were compared, using voxel-wise cross-participant statistics with a paired  $t$  test within the FSL randomize tool (version 2.1, 5000 permutations). Correction of multiple comparisons was carried out using the threshold-free cluster enhancement (TFCE) method.<sup>17</sup>

A mask separating the WM pathways was manually created with ITK-SNAP ([www.itksnap.org](http://www.itksnap.org))<sup>18</sup>, using the FA-skeletonized data.  $P$  values were then extracted for each WM tract. The pathways were identified, using FSLview integrated atlases JHU ICBM-DTI81 White-Matter Labels and JHU White-Matter Tractography Atlas. We also utilized anatomist from the BrainVisa toolbox ([www.brainvisa.info](http://www.brainvisa.info)) and homemade scripts for verification and visualization.

The WM pathways of interest were those purported to be involved in attentional processes. The pathways connect the frontoparietal networks (eg, superior longitudinal fasciculus [SLF], inferior longitudinal fasciculus [ILF], and cingulum bundle [CB]), or are implicated in interhemispheric processing within parietal areas (eg, splenium of the corpus callosum [SCC]).<sup>19,20</sup>

### Gray Matter/VBM

The GM analysis was conducted using FSL-VBM, a VBM style analysis<sup>21,22</sup> with FSL tools.<sup>23</sup> Structural images were brain-extracted using BET.<sup>14</sup> Segmentation was then carried out using FAST4.<sup>24</sup> The resulting GM partial volume images were then aligned to the MNI152 standard space using the affine registration tool FLIRT,<sup>25,26</sup> which was followed by a nonlinear registration using FNIRT<sup>27,28</sup> (this program uses a b-spline representation of the registration warp field<sup>29</sup>). Images were then averaged to create a study-specific template, to which the native GM images were then nonlinearly reregistered. The registered partial volume images were then modulated (to correct for local expansion or contraction) by

dividing using the Jacobian of the warp field (this procedure allows to compare the absolute amount of tissue). The modulated segmented images were then smoothed with an isotropic Gaussian kernel (full width at half maximum = 7 mm). Finally, regions were extracted from FreeSurfer gyri atlas<sup>30,31</sup> and a voxel-wise GLM TFCE-based analysis, permutation-based nonparametric testing (5000 permutations), and correction for multiple comparisons across space. A homemade script was then used to extract the number of significant voxels in each region. For each group, GMV changes between Time 1 and Time 2 were assessed using a paired  $t$  test. Based on previous studies, and given the exploratory nature of the present investigation, a lower height threshold ( $P < .05$  cluster uncorrected for whole brain, minimum cluster size: 5 or more voxels) was accepted for the following regions of interest: inferior, middle, and superior frontal gyri; SPL; inferior and superior temporal gyri; and thalamus (THAL). These cortical regions were selected on the basis of their previously demonstrated involvement in sustained attention and the location of the training electrodes.

### Measurement of Attentional Performance

The attentional performance of all participants was assessed at Time 1 and Time 2 using the Integrated Visual Auditory (IVA) continuous performance test (BrainTrain, 727 Twin Ridge Lane, Richmond, Virginia<sup>32</sup>). This computerized, continuous test measures mostly sustained attention and combines 2 types of continuous performance subtests for visual and auditory modalities. During the IVA, “1”s and “2”s were presented in a pseudorandom combination of visual and auditory stimuli. The participants were requested to click the computer mouse only when they heard or saw the target (the number 1), and not to click when they saw or heard the nontarget item (the number 2). This test lasted for 15 minutes. For each group of participants, the scores on the IVA at Time 2 and Time 1 were compared using a paired  $t$  test.

## Results

### The IVA Data

In the EXP group, the scores on the IVA full scale attention quotient (which is based on measures of both visual and auditory attention) significantly increased at Time 2, compared to Time 1 ( $P < .005$ ). Scores on auditory attention were also significantly higher ( $P < .005$ ) following NFT. For participants in the SHAM group, scores on visual attention were greater ( $P < .005$ ) at Time 2 relative to Time 1. No difference in attentional performance was noted at Time 2, compared to Time 1, for members of the CON group.

### The FA Changes in WM Pathways Following NFT

With respect to DTI data, in the EXP group, comparisons between Time 2 and Time 1 scans revealed significant increases in FA in the right CB ( $x = 12, y = -11, z = 31$ ;  $P < .05$  corrected), right anterior corona radiata (ACR;  $x = 24, y = 22, z = 20$ ;  $P < .05$  corrected), and the SCC ( $x =$

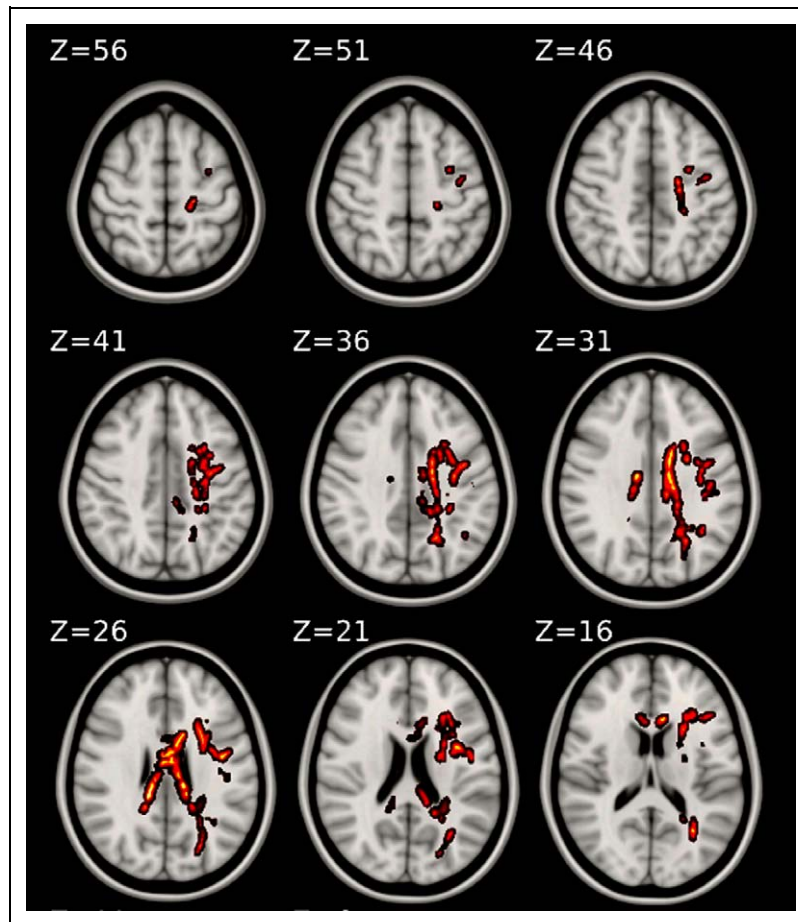


**Figure 1.** Significant increase in fractional anisotropy ([FA] displayed in red-yellow) in white matter pathways following neurofeedback training (NFT). The horizontal background T1-weighted images are sections of the MNI template shown in radiological convention.

$-14, y = -26, z = 27; P < .05$  corrected). Increased FA was also measured in the left SLF ( $x = -33, y = -9, z = 33; P < .05$  corrected), left ILF ( $x = -26, y = -58, z = 33; P < .05$  corrected), left anterior limb of the internal capsule (ALIC;  $x = -20, y = 15, z = 10; P < .05$  corrected), and left CB ( $x = -20, y = -52, z = 35; P < .05$  corrected; see Figure 1).

Post hoc analyses revealed positive correlations between enhanced visual attention score and increases in FA in the left SLF ( $r = .68, P < .05$ ) and the left ALIC ( $r = .66, P < .05$ ).

In SHAM and CON groups, no significant change in FA was measured at Time 2, relative to Time 1, with regard to WM pathways.

### The GMV Alterations Related to NFT

At Time 2 compared to Time 1, significant GMV increases were found in the EXP group in the right middle frontal gyrus (MFG;  $x = 26, y = 32, z = 50$ ; Brodmann area [BA] 9;  $P < .01$ ; size: 5 voxels; and  $x = 48, y = 2, z = 52$ ; BA 6;  $P < .01$ ; size: 7), right inferior temporal gyrus (ITG;  $x = 50, y = -26, z = -32$ ; BA 20;  $P < .01$ ; size: 8), right middle occipital gyrus (MOG;  $x = 46, y = -86, z = -10$ ; BA 19;  $P < .01$ ; size: 132), and right THAL ( $x = 16, y = -22, z = 18; P < .05$ ; size: 99). Increased

GMV was also noted in the left superior frontal gyrus (SFG;  $x = -22, y = 8, z = 68$ ; BA 6;  $P < .01$ ; size: 12), left inferior frontal gyrus (IFG;  $x = -54, y = 28, z = -6$ ; BA 47;  $P < .01$ ; size: 238), left superior temporal gyrus (STG;  $x = -50, y = 16, z = -6$ ; BA 22;  $P < .01$ ; size: 190), and left SPL ( $x = -28, y = -86, z = 42$ ; BA 7;  $P < .01$ ; size: 19; see Figure 2).

In SHAM group, GMV increases were measured in the right MFG ( $x = 34, y = 52, z = 28$ ; BA 10;  $P < .01$ ; size: 79) and SFG ( $x = 10, y = 14, z = 72$ ; BA 6;  $P < .01$ ; size: 13). Increased GMV was also detected in the left MFG ( $x = -42, y = 50, z = 16$ ; BA 10;  $P < .01$ ; size: 28), left cuneus ( $x = -12, y = -106, z = 4$ ; BA 18;  $P < .01$ ; size: 222), and left THAL ( $x = -4, y = -6, z = 12; P < .01$ ; size: 77; see Figure 3).

No change in GM was noted for members of the CON group.

### Discussion

In agreement with the results of our previous studies,<sup>3,4</sup> increasing  $\beta 1$  frequency band via NFT significantly enhanced visual and auditory sustained attention performance (as measured with the IVA). This finding provides further support for the view that there is a functional relationship between  $\beta 1$

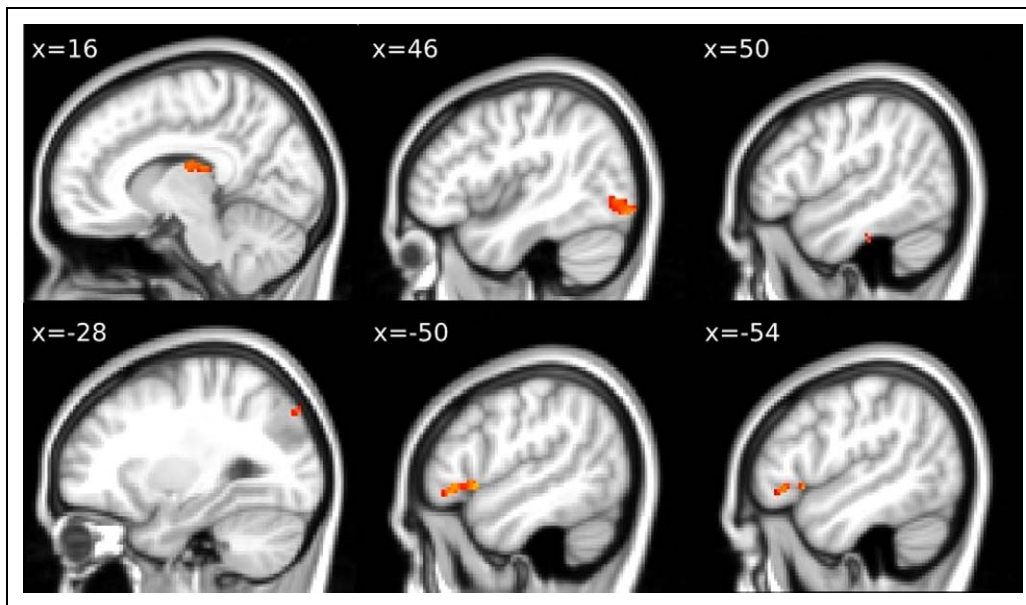


**Figure 2.** Increases in gray matter volume (GMV) found in the experimental (EXP) group following neurofeedback training (NFT).

activity and sustained attention.<sup>5,6</sup> It is noteworthy that scores on sustained visual attention increased at Time 2, relative to Time 1, in the SHAM group. No difference in attentional performance was noted at Time 2, compared to Time 1, in the CON group. Given this, it seems likely that this improvement in sustained visual attention is related to the fact that for approximately 20 hours, participants in the SHAM group had to undergo a perceptual-cognitive “training”, consisting of staring at the computer screen and staying focused with respect to the animation displayed on that screen. The members of this group also received hours of personal coaching to pay attention visually.

Increased FA values of the right CB, right ACR, and SCC were found in the EXP group following NFT. The results are particularly striking considering that these WM pathways are known to be associated with sustained attention.<sup>33–35</sup> The CB connects the anterior cingulate cortex with the dorsolateral prefrontal cortex (DLPFC) and the posterior portion of the parietal cortex. Relative to healthy controls, smaller FA values have been reported in the CB in adults with childhood ADHD.<sup>36</sup> Moreover, decreased FA has been found in the ACR—which connects the frontal cortex and the brainstem—in children and adolescents with this developmental disorder.<sup>37,38</sup> As for the SCC, this tract may be implicated in the coordination of inter-hemispheric processing across parietal areas that are part of attention networks.<sup>20</sup> A volumetric reduction of this posterior area of the corpus callosum is one of the most consistent findings in children with ADHD.<sup>39</sup> In addition, DTI studies have reported lower FA in the SCC in individuals with ADHD, compared to healthy people.<sup>38</sup>

In the left hemisphere, NFT also led to increased FA in the CB, SLF, ILF, and ALIC. Furthermore at Time 2, positive correlations were found between enhanced visual attention scores and increases in FA in the left SLF and left ALIC. These results might seem a bit peculiar at first blush. Indeed, frontal

and parietal cortical areas, located predominantly in the right hemisphere, have been most frequently found to be activated in response to sustaining attention tasks in visual, auditory, and somatosensory modalities.<sup>7,8</sup> Nonetheless, there is electrophysiological (EEG),<sup>40</sup> clinical neuropsychological,<sup>41</sup> and functional neuroimaging data (see the references below) indicating that the left hemisphere is implicated in sustained attention.

The SLF and ILF are putatively involved in the transmission of information between frontal and posterior areas of the brain.<sup>34</sup> Anatomically, the SLF runs between superior frontal and parietal areas. This pathway is believed to provide a means enabling the prefrontal cortex to supervise the allocation of attentional resources.<sup>42</sup> In regard to the ILF, this tract traverses frontotemporal and occipitoparietal regions and is part of the visual attentional network. In regard to the ALIC, this pathway contains fibers connecting the THAL with the DLPFC.<sup>43</sup>

Recently, a DTI study conducted in healthy participants demonstrated a positive correlation between FA values in the ALIC and performance on a sustained attention task.<sup>19</sup> Moreover, in line with the results of the present study, other DTI investigations carried out in individuals with ADHD have evidenced significantly reduced FA values, in the left hemisphere, in the CB, SLF, ILF, and ALIC.<sup>37,38,44,45</sup>

As already noted, F4 corresponds to the right middle and superior frontal gyri, whereas P4 corresponds to the right posterior superior area of the parietal lobe, according to the 3D probabilistic anatomical craniocerebral correlation.<sup>13</sup> Because of this, it is conceivable that the simultaneous training of  $\beta 1$  activity at F4 and P4 in the EXP group stimulated neuronal communication between frontal and parietal regions within the right hemisphere and between homologous frontal and parietal regions in both the hemispheres.

Following NFT, GMV increases were found in the EXP group in the right (MFG BA 9, inferior temporal gyrus (ITG)



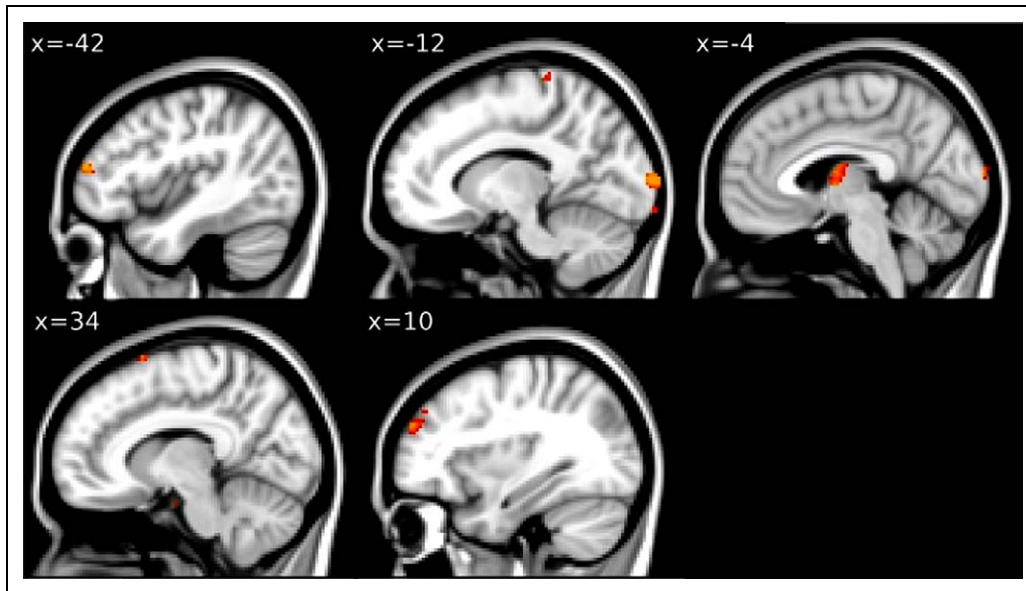


**Figure 3.** Regions that showed a gray matter volume (GMV) increase at Time 2 (relative to Time 1) in the SHAM group.

BA 20, MOG BA 19, THAL) and left (SFG BA6, IFG BA 47, STG BA 22, SPL BA 7) hemispheres. Interestingly, these brain regions have been shown activated, in the right and/or left hemispheres, during various types of sustained attention tasks.<sup>46–54</sup> The MFG and the SFG may mediate attentional control,<sup>7</sup> whereas the IFG and the THAL may be linked to the regulation of vigilance. Other lines of evidence suggest that the ITG plays a crucial role in the analysis complex images,<sup>55</sup> whereas the STG seems to be involved in auditory sustained attention.<sup>53</sup> As for the SPL, it has been proposed that this component of the posterior attentional system is associated with visual vigilance.<sup>46,49</sup>

Intriguingly, at Time 2 compared to Time 1, GMV increases were detected in the SHAM group in the right MFG (BA 10), right SFG (BA 6), left MFG (BA 10), left cuneus, and left THAL. It appears reasonable to assume that these GMV increases were somehow related to the perceptual and cognitive processes associated with the sham procedure, and to personal coaching of visual attention. It should be noted here that the GMV changes seen in the SHAM group were not as robust or extensive as those observed in the EXP group. Furthermore, the fact that the sham condition produced GM and performance changes in the direction of the experimental effects, suggests that it may be difficult to isolate the impact of NFT protocols in randomized controlled trials.

A recent investigation showed that EEG-based NFT can lead to changes in human cortical excitability.<sup>56</sup> Given this, the NFT protocol used in this study might have enhanced neural transmission in networks mediating sustained attention. It has been proposed that alterations in WM microstructural properties might support cognitive enhancement by changing conduction velocity.<sup>57</sup> Additionally, it has been demonstrated that electrical activity within an axon can modulate its myelination over a period of weeks.<sup>58,59</sup> In other respects, there is evidence

that myelination is still sensitive to experience during adulthood.<sup>60</sup> In this context, it is possible that NFT led to enhanced conduction velocity in sustained attention-related neural networks which, in turn, increased the myelination of axons in these networks.

The cellular processes mediating the GMV increases in cerebral structures associated with sustained attention remain unclear at this time. Regarding this question, synaptogenesis<sup>61</sup> and changes in dendritic spine morphology<sup>62</sup> have been shown to be associated with motor skill learning in rodents. In view of these findings, it does not seem too farfetched to speculate that the GMV changes measured at Time 2 might have been related to alterations in synaptogenesis and/or spine formation.

The main limitation of this study is the small sample size. Given this, the present results should be interpreted with caution until being replicated in larger samples. Despite this limitation, however, FA increases in WM pathways were relatively robust following NFT. Another limitation is related to the fact that for the VBM analysis, an uncorrected threshold of  $P < .05$  was used (such a threshold has been utilized in previous exploratory VBM studies). Nevertheless, in the EXP group, the GMV increases induced by NFT were found in areas involved in sustained attention. In our view, this is quite revealing, especially given the rather small sample size of this investigation.

In summary, our results show that a NFT protocol aimed at enhancing  $\beta 1$  activity can enhance visual and auditory sustained attention performance. Importantly, our results indicate that this protocol can induce modifications in WM pathways implicated in sustained attention. Furthermore, such a protocol can produce GMV alterations in brain regions involved in this kind of attention. After 50 years of research in the field of neurofeedback, our study constitutes the first empirical demonstration that NFT can lead to microstructural changes in WM and GM.

It is remarkable that our results were obtained from training “normal” healthy individuals. One may wonder whether NFT could lead to even greater changes in clinical populations. Regarding this question, it would be important to replicate this study with clinical and EEG subtypes of attention deficit disorder/ADHD.

### Acknowledgments

We thank the staff of the Neuroimaging Unit, Centre de recherche du Centre hospitalier de l'Université de Montréal (CRCHUM, Hôpital Notre-Dame) for their technical assistance.

### Declaration of Conflicting Interests

The author(s) declared no potential conflicts of interest with respect to the research, authorship, and/or publication of this article.

### Funding

The author(s) disclosed receipt of the following financial support for the research, authorship, and/or publication of this article: a research grant from the Foundation Denis Guichard (Paris, France) to M. B.

### References

1. Monastra VJ, Lynn S, Linden M, Lubar JF, Gruzelier J, LaVaque TJ. Electroencephalographic biofeedback in the treatment of attention-deficit/hyperactivity disorder. *Appl Psychophysiol Biofeed*. 2005;30(2):95-114.
2. Arns M, de Ridder S, Strehl U, Breteler M, Coenen A. Efficacy of neurofeedback treatment in ADHD: the effects on inattention, impulsivity and hyperactivity: a meta-analysis. *Clin EEG Neurosci*. 2009;40(3):180-189.
3. Beauregard M, Lévesque J. Functional magnetic resonance imaging investigation of the effects of neurofeedback training on the neural bases of selective attention and response inhibition in children with attention-deficit/hyperactivity disorder. *Appl Psychophysiol Biofeed*. 2006;31(1):3-20.
4. Lévesque J, Beauregard M, Mensour B. Effect of neurofeedback training on the neural substrates of selective attention in children with attention-deficit/hyperactivity disorder: a functional magnetic resonance imaging study. *Neurosci Lett*. 2006;394(3):216-221.
5. Molteni E, Bianchi AM, Butti M, Reni G, Zucca C. Analysis of the dynamical behaviour of the EEG rhythms during a test of sustained attention. *Conf Proc IEEE Eng Med Biol Soc*. 2007; 1298-1301.
6. Arruda JE, Zhang H, Amoss RT, Coburn KL, Aue WR. Rhythmic oscillations in quantitative EEG measured during a continuous performance task. *Appl Psychophysiol Biofeed*. 2009;34(1):7-16.
7. Coull JT. Neural correlates of attention and arousal: insights from electrophysiology, functional neuroimaging, and psychopharmacology. *Prog Neurobiol*. 1998;55(4):343-361.
8. Sarter M, Givens B, Bruno JP. The cognitive neuroscience of sustained attention: where top-down meets bottom-up. *Brain Res Rev*. 2001;35(2):146-160.
9. Takeuchi H, Sekiguchi A, Taki Y, et al. Training of working memory impacts structural connectivity. *J Neurosci*. 2010; 30(9):3297-3303.
10. Beaulieu C. The biological basis of diffusion anisotropy. In: Johansen-Berg H, Behrens TEJ, eds. *Diffusion MRI: From Quantitative Measurement to In Vivo Neuroanatomy*. London, England: Elsevier; 2009:105-126.
11. Lee B, Park JY, Jung WH, et al. White matter neuroplastic changes in long-term trained players of the game of "Baduk" (GO): a voxel-based diffusion-tensor imaging study. *NeuroImage*. 2010;52(1):9-19.
12. Ceccarelli A, Rocca MA, Pagani E, Falini A, Comi G, Filippi M. Cognitive learning is associated with gray matter changes in healthy human individuals: a tensor-based morphometry study. *NeuroImage*. 2009;48(3):585-589.
13. Okamoto M, Dan H, Sakamoto K, et al. Three-dimensional probabilistic anatomical cranio-cerebral correlation via the international 10-20 system oriented for transcranial functional brain mapping. *NeuroImage*. 2004;21(1):99-111.
14. Smith SM. Fast robust automated brain extraction. *Hum Brain Map*. 2002;17(3):143-155.
15. Jenkinson M, Pechaud M, Smith S. BET2: MR-based estimation of brain skull and scalp surfaces. Eleventh Annual Meeting of the Organization for Human Brain Mapping; 2005.
16. Smith SM, Jenkinson M, Johansen-Berg H, et al. Tract-based spatial statistics: voxelwise analysis of multi-subject diffusion data. *NeuroImage*. 2006;31(4):1487-1505.
17. Smith SM, Nichols ET. Thresholding-free cluster enhancement: addressing problems of smoothing, threshold dependence and localisation in cluster interference. *NeuroImage*. 2009;44(1):83-98.
18. Yushkevich AP, Piven J, Hazlett CH, et al. User-guided 3D active contour segmentation of anatomical structures: Significantly improved efficiency and reliability. *NeuroImage*. 2006;31(3): 1116-1128.
19. Niogi S, Mukherjee P, Ghajar J, McCandliss BD. Individual differences in distinct components of attention are linked to anatomical variations in distinct white matter tracts. *Front Neuroanat*. 2010;4:2.
20. Bennett IJ, Motes MA, Rao NK, Rypma B. White matter tract integrity predicts visual search performance in young and older adults. *Neurobiol Aging*. 2012;33(2):433.e21-431.
21. Ashburner J, Friston K. Voxel-based morphometry – the methods. *NeuroImage*. 2000;14(6 pt 1):21-36.
22. Good C, Johnsrude I, Ashburner J, Henson R, Friston K, Frackowiak R. A voxel-based morphometric study of ageing in 465 normal adult human brains. *NeuroImage*. 2001;14(1 pt 1):21-36.
23. Smith SM, Jenkinson M, Woolrich MW, et al. Advances in functional and structural MR image analysis and implementation as FSL. *NeuroImage*. 2004;23:208-219.
24. Zhang Y, Brady M, Smith SM. Segmentation of brain MR images through a hidden Markov random field model and the expectation maximization algorithm. *IEEE Trans Med Imaging*. 2001;20(1):45-57.
25. Jenkinson M, Smith SM. A global optimisation method for robust affine registration of brain images. *Med Imaging*. 2001;5(2):143-156.
26. Jenkinson M, Bannister PR, Brady JM, Smith SM. Improved optimisation for the robust and accurate linear registration and motion correction of brain images. *NeuroImage*. 2002;17(2):825-841.
27. Andersson JLR, Jenkinson M, Smith SM. Non-linear optimisation. FMRIB technical report TR07JA1. 2007. www.fmrib.ox.ac.uk/analysis/techrep. (accessed on July 14, 2012).



28. Andersson JLR, Jenkinson M, Smith SM. Non-linear registration, aka Spatial normalisation. FMRIB technical report TR07JA2. 2007. www.fmrib.ox.ac.uk/analysis/techrep. (accessed on July 14, 2012).
29. Rueckert D, Sonoda LI, Hayes C, Hill DLG, Leach MO, Hawkes DJ. Nonrigid registration using free-form deformations: application to breast MR images. *IEEE Trans Med Imaging*. 1999; 18(8):712-721.
30. Desikan RS, Segonne F, Fischl B, et al. An automated labeling system for subdividing the human cerebral cortex on MRI scans into gyral based regions of interest. *NeuroImage*. 2006;31(3):968-980.
31. Fischl B, van der Kouwe A, Destrieux C, et al. Automatically parcellating the human cerebral cortex. *Cerebr Cort*. 2004;14(1):11-22.
32. Tinius TP. The integrated visual and auditory continuous performance test as a neuropsychological measure. *Arch Clin Neuropsychol*. 2003;18(5):439-454.
33. Mesulam MM. Large-scale neurocognitive networks and distributed processing for attention, language, and memory. *Ann Neurol*. 1990;28(5):597-613.
34. Makris N, Buka SL, Biederman J, et al. Attention and executive systems abnormalities in adults with childhood ADHD: a DTMRI study of connections. *Cerebr Cortex*. 2008;18(5):1210-1220.
35. Takahashi M, Iwamoto K, Fukatsu H, Naganawa S, Iidaka T, Ozaki N. White matter microstructure of the cingulum and cerebellar peduncle is related to sustained attention and working memory: a diffusion tensor imaging study. *Neurosci Lett*. 2010; 477(2):72-76.
36. Makris N, Biederman J, Monuteaux MC, Seidman LJ. Towards conceptualizing a neural systems-based anatomy of attention-deficit/hyperactivity disorder. *Develop Neurosci*. 2009;21(1-2):36-49.
37. Pavuluri MN, Yang S, Kamineni K, et al. Diffusion tensor imaging study of white matter fiber tracts in pediatric bipolar disorder and attention-deficit/hyperactivity disorder. *Biol Psychiatry*. 2009;65(7):586-593.
38. Qiu MG, Ye Z, Li QY, Liu GJ, Xie B, Wang J. Changes of brain structure and function in ADHD children. *Brain Topogr*. 2011; 24(3-4):243-252.
39. Valera EM, Faraone SV, Murray KE, Seidman LJ. Meta-analysis of structural imaging findings in ADHD. *Biol Psychiatry*. 2007; 61(12):1361-1369.
40. Kelly SP, Lalor EC, Reilly RB, Foxe JJ. Increases in alpha oscillatory power reflect an active retinotopic mechanism for distracter suppression during sustained visuospatial attention. *J Neurophysiol*. 2006;95(6):3844-3851.
41. Audet T, Mercier L, Collard S, Rochette A, Hébert R. Attention deficits: is there a right hemisphere specialization for simple reaction time, sustained attention, and phasic alertness? *Brain Cogn*. 2000;43(1-3):17-21.
42. Mesulam MM. Attentional networks, confusional states, and neglect syndromes. In: Mesulam MM, ed. *Principles of Behavioral and Cognitive Neurology*. 2nd ed. Oxford, England: Oxford University Press; 2000:174-256.
43. Parent A. *Carpenter's Human Neuroanatomy*. 9th ed. Baltimore, MD: Williams & Wilkins; 1996.
44. Hamilton LS, Levitt JG, O'Neill J, et al. Reduced white matter integrity in attention-deficit hyperactivity disorder. *Neuroreport*. 2008;19(17):1705-1708.
45. Konrad A, Dielentheis TF, Masri DE, et al. White matter abnormalities and their impact on attentional performance in adult attention-deficit/hyperactivity disorder. *Eur Arch Psychiatry Clin Neurosci*. 2012;262(4):351-360.
46. Pardo JV, Fox PT, Raichle ME. Localization of a human system for sustained attention by positron emission tomography. *Nature*. 1991;349(630):61-64.
47. Coull JT, Frith CD, Frackowiak RS, Grasby PM. A fronto-parietal network for rapid visual information processing: a PET study of sustained attention and working memory. *Neuropsychology*. 1996;34(11):1085-1095.
48. Johannsen P, Jakobsen J, Bruhn P, et al. Cortical sites of sustained and divided attention in normal elderly humans. *NeuroImage*. 1997;6(3):145-155.
49. Vandenberghe R, Gitelman DR, Parrish TB, Mesulam MM. Functional specificity of superior parietal mediation of spatial shifting. *NeuroImage*. 2001;14(3):661-673.
50. Lawrence NS, Ross TJ, Hoffmann R, Garavan H, Stein EA. Multiple neuronal networks mediate sustained attention. *J Cogn Neurosci*. 2003;15(7):1028-1038.
51. Kim J, Whyte J, Wang J, Rao H, Tang KZ, Detre JA. Continuous ASL perfusion fMRI investigation of higher cognition: quantification of tonic CBF changes during sustained attention and working memory tasks. *NeuroImage*. 2006;31(1):376-385.
52. Epstein JN, Delbello MP, Adler CM, et al. Differential patterns of brain activation over time in adolescents with and without attention deficit/hyperactivity disorder (ADHD) during performance of a sustained attention task. *Neuropediatrics*. 2009;40(1):1-5.
53. Saupe K, Schröger E, Andersen SK, Müller MM. Neural mechanisms of intermodal sustained selective attention with concurrently presented auditory and visual stimuli. *Front Hum Neurosci*. 2009;3:58.
54. Tana MG, Montin E, Cerutti S, Bianchi AM. Exploring cortical attentional system by using fMRI during a continuous performance test. *Computat Intell Neurosci*. 2010;329213. doi:10.1155/2010/329213.
55. Anderson B, Mruczek RE, Kawasaki K, Sheinberg D. Effects of familiarity on neural activity in monkey inferior temporal lobe. *Cerebr Cortex*. 2008;18(11):2540-2552.
56. Ros T, Munneke MA, Ruge D, Gruzeliér JH, Rothwell JC. Endogenous control of waking brain rhythms induces neuroplasticity in humans. *Eur J Neurosci*. 2010;31(4):770-778.
57. Fields RD. White matter in learning, cognition and psychiatric disorders. *Trends Neurosci*. 2008;31(7):361-370.
58. Demerens C, Stankoff B, Logak M, et al. Induction of myelination in the central nervous system by electrical activity. *Proc Natl Acad Sci U S A*. 1996;93(18):9887-9892.
59. Ishibashi T, Dakin KA, Stevens B, et al. Astrocytes promote myelination in response to electrical impulses. *Neuron*. 2006; 49(6):823-832.
60. Markham JA, Greenough WT. Experience-driven brain plasticity: beyond the synapse. *Neuron Glia Biol*. 2004;1(4):351-363.
61. Kleim JA, Barbay S, Cooper NR, et al. Motor learning-dependent synaptogenesis is localized to functionally reorganized motor cortex. *Neurobiol Learn Mem*. 2002;77(1):63-77.
62. Kolb B, Cioe J, Comeau W. Contrasting effects of motor and visual spatial learning tasks on dendritic arborization and spine density in rats. *Neurobiol Learn Mem*. 2008;90(2):295-300.